JOURNAL OF MATERIALS SCIENCE 28 (1993) 719–728

Densification and microstructure development during the sintering of submicrometre magnesium oxide particles prepared by a vapour-phase oxidation process

K. ITATANI, A. ITOH, F. S. HOWELL, A. KISHIOKA, M. KINOSHITA
Department of Chemistry, Faculty of Science and Technology, Sophia University, 7-1 Kioi-cho, Chiyoda-ku, Tokyo 102 Japan

The densification behaviour and microstructure development of MgO compacts fired from room temperature up to 1700 °C at a heating rate of 10 °C min^{-1} were examined. Starting materials were seven kinds of MgO powder with primary particle sizes ranging from 11–261 nm; these powders were produced by a vapour-phase oxidation process. The original powders contained agglomerates, due to the spontaneous coagulation of primary particles, which ranged in size from 100–500 nm. The MgO compacts densified during firing by three types of sintering: sintering within agglomerates; sintering between agglomerates and grains; and rearrangement of agglomerates and grains. The MgO compact with the lowest primary particle size (11 nm) densified by the first and second types of sintering, but the effects of these two types of sintering decreased when the primary particle size became 44 nm; here the rearrangement of agglomerates and grains primarily contributed to densification of the compact. All three types of densification became less complete with further increases in primary particle size up to 261 nm. The relative densities of the MgO compacts with smaller primary particle sizes (11–44 nm) became 96–98% when the compacts were fired up to 1700 °C.

1. Introduction

Submicrometre magnesium oxide (MgO) particles have begun to be produced recently by many advanced techniques [1–4]. Among these, the vapour-phase oxidation process (VPO-P) [4] is a unique technique for synthesis of MgO powder with the following properties [5] : (i) high purity (over 99.9%), (ii) free from hard agglomerates, and (iii) narrow particle size distribution.

The sinterability of ultrafine MgO powder (primary particle size 10–20 nm) synthesized by VPO-P has been reported by some researchers. Watari *et al.* [6] found that the sintered MgO compact with relative density of ~97% can easily be fabricated by firing the compressed powder at a temperature as low as 1400 °C. The densification and changes in microstructure during the firing of MgO compact were examined quantitatively by the present authors [7] ; more extensive information was obtained by Nishida *et al.* [8], who examined the sinterabilities of MgO powders with different primary particle sizes from 10–200 nm.

As shown above, the sintered MgO compact with a relative density of ~97% can be fabricated by using an MgO powder synthesized by VPO-P. In spite of these results, however, the effect of primary particle size on densification and microstructure development during the firing of MgO compact has not yet been examined in detail.

This paper describes the densification behaviour and microstructure development during the sintering of submicrometre MgO particles with the primary particle sizes of 11–261 nm synthesized by VPO-P.

2. Experimental procedure

2.1. Starting materials and preparation of compacts

Seven kinds of MgO powder with average primary particle sizes from 11–261 nm were supplied by Ube Industries. About 1.5–2.0 g MgO powder was pressed uniaxially at 39 MPa into a compact (20 mm diameter and 3 mm thick); here the compaction–fracture operation was repeated twice to fabricate a dense and uniform compact.

2.2. Measurements of specific surface area, crystallite size and primary particle size

The specific surface area of the original MgO powder was measured by the BET technique, using nitrogen as an adsorption gas.

0022–2461

The crystallite size, G_{XRD}, of each original MgO powder was calculated using Scherrer's formula, using an X-ray diffractometer (40 kV, 25 mA) with nickel-filtered CuK_α radiation (Model RADII A, Rigaku, Tokyo)

$$G_{XRD} = \frac{K\lambda}{\beta\cos\theta} \quad (1)$$

where λ is a wavelength of CuK_{α_1} (= 0.15405 nm), β a half-width of the (4 2 0) reflection, θ a Bragg angle and K a constant (= 0.9).

The primary particle size, G_{BET}, was calculated using the following equation, assuming that the particle shape was cubic

$$G_{BET} = \frac{F}{\rho S} \quad (2)$$

where ρ is the theoretical density (= 3.595 g cm^{-3}), S the specific surface area and F a particle-shape factor (= 6).

2.3. Measurement of relative density of MgO compact

The relative density of each MgO compact was calculated by dividing the bulk density by the theoretical density. The bulk density of each MgO compact was calculated by measuring the dimensions and weight of the compact.

2.4. Observation of particle and grain shapes

The particle shape of each MgO powder was observed by transmission electron microscopy (TEM; Model H-300, Hitachi, Tokyo).

The grain shape was observed by scanning electron microscopy (SEM; Model S-430, Hitachi, Tokyo), after the sintered compact had been polished and then thermally etched.

2.5. Measurement of grain size in sintered MgO compact

The grain size of the sintered MgO compact was measured as follows [9] : after drawing lines at regular intervals on the scanning electron micrographs, the grain sizes were obtained by multiplying $\pi/2$ times the measured values of the distance between grain boundaries on the lines. About 400–500 grains were counted in each measurement.

3. Results and discussion

3.1. Properties of MgO powder prepared by VPO-P

The chemical analyses of MgO powders were performed by Ube Industries. The purities of these MgO powders were over 99.98%; the impurities in these MgO powders were SiO_2 (< 0.005%), CaO (< 0.004%), Al_2O_3 (< 0.003%), ZnO (< 0.003%), Fe_2O_3 (< 0.003%), Na_2O (< 0.001%), MnO (< 0.001%) and U + Th (< 1 p.p.b.).

The crystallite sizes, G_{XRD}, primary particle sizes, G_{BET}, and degrees of agglomerations, $(G_{BET}/G_{XRD})^3$, of MgO powders are shown in Table I, together with the particle shapes observed by TEM; here the seven kinds of MgO powder are abbreviated as Powders A(11) to G(261). The shapes of these MgO particles were chiefly cubic but partly round-cornered. The crystallite sizes of these MgO powders were almost in accord with the primary particle sizes; thus the degrees of agglomerations of these MgO powders were found to be nearly unity.

The above results suggest that the primary particles are composed of single crystals [10]. The same results have been obtained by Watari *et al.* [6], who confirmed that the average particle size observed by TEM agrees with the crystallite size measured by an X-ray diffraction technique (XRD-T).

3.2. Densification behaviour of MgO compact

The relative density of each sintered MgO compact was measured to evaluate the degree of the densification. Results are shown in Fig. 1. The densification behaviour during the firing of MgO compacts could be divided into five categories: (i) Compact A(11), (ii) Compacts B(25) and C(32), (iii) Compact D(44), (iv) Compact E(57), (v) Compacts F(107) and G(261). The densification behaviour of the MgO compact(s) in each category is explained below.

3.2.1. Compact A(11)

The relative density was only 38.3% at 600 °C; however, it rose rapidly with increasing temperatures and attained 97.8% at 1700 °C. A marked increase in relative density, i.e. 70%–90%, was observed on increasing the temperature from 1300 °C to 1400 °C.

3.2.2. Compacts B(25) and C(32)

The densifications proceeded more slowly than that of Compact A(11). For example, the temperature at which the relative density increased from 66–70% to

TABLE I Some properties of MgO powders synthesized by VPO-P

Sample[a]	Crystallite (nm)	Primary particle (nm)	Degree of agglomeration[b]	Shape of particles[c]
A(11)	11	11	1.0	Cubic
B(25)	24	25	1.1	Cubic
C(32)	32	32	1.0	Cubic
D(44)	41	44	1.2	Cubic
E(57)	57	57	1.0	Cubic
F(107)	103	107	1.1	Cubic[d]
G(261)	257	261	1.1	Cubic[d]

[a] Figures in parentheses indicate the primary particle sizes.
[b] The degree of agglomeration was obtained by cubing the quotient of primary particle size divided by crystallite size.
[c] The particle shape was observed by TEM.
[d] The cubic particles with rounded corners were also present in the powder.

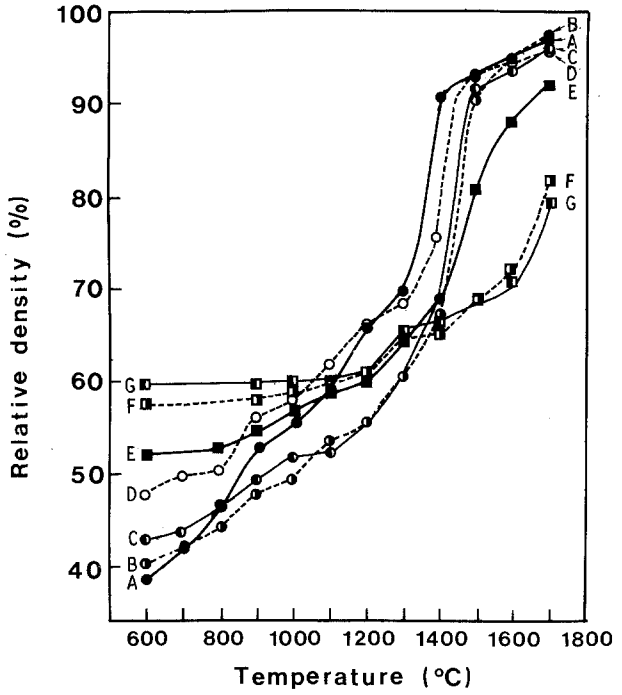

Figure 1 Changes in relative densities during the firing of MgO compacts up to 1700 °C (heating rate 10 °C min^{-1}). A to G: Compacts A(11) to G(261).

~91% (1400–1500 °C) was about 100 °C higher than that of Compact A(11). The relative densities of Compacts B(25) and C(32) at 1700 °C were 97.9% and 96.8%, respectively.

3.2.3. Compact D(44)

The densification behaviour was analogous to that of Compact A(11), except for that in the range 600–800 °C. The relative density attained 96.6% at 1700 °C.

3.2.4. Compact E(57)

Although the densification was enhanced on increasing the temperature to 1500 °C, it became slower on further firing up to 1700 °C. The relative density attained 92.8% at 1700 °C.

3.2.5. Compacts F(107) and G(261)

The relative densities did not change markedly between 600 and 1100 °C; however, they increased gradually and attained 79%–82% at 1700 °C.

The relative densities of Compacts A(11) to G(261) at 1700 °C are arranged as follows: Compact A(11) (97.8%) ≈ Compact B(25) (97.9%) > Compact C(32) (96.8%) ≈ compact D(44) (96.6%) > Compact E(57) (92.8%) > Compact F(107) (81.9%) > Compact G(261) (79.4%). The overall trend reveals that the smaller is the original primary particle size, the higher the relative density becomes.

In order to clarify the effect of primary particle size on sintering of MgO powder, the relative densities of sintered MgO compacts were plotted against the original primary particle sizes. Results are shown in Fig. 2, together with the relative densities of the green

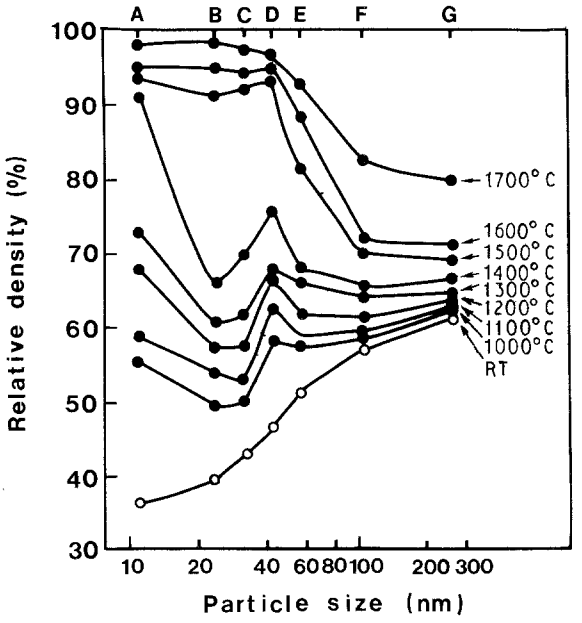

Figure 2 Relationship between original primary particle size and relative density. RT = room temperature. A to G: Compacts A(11) to G(261).

MgO compacts. The green relative densities increased from 36.5% (Compact A(11)) to 60.7% (Compact G(261)) with increasing primary particle size. The increasing behaviour of relative densities of MgO compacts could be divided into two categories, according to the firing temperature, i.e. 1000–1400 °C and 1500–1700 °C. The isothermal relative density curves in the range 1000–1400 °C appeared to be w-type; for example, the relative densities of Compacts A(11) and D(44) fired to 1400 °C, which corresponded to 91.0% and 75.5%, respectively, became higher than those (65.0%–69.0%) of other compacts. On the other hand, the isothermal relative density curves in the range of 1500–1700 °C showed that the relative densities of Compacts A(11) to D(44) were higher than those of Compacts E(57) to G(261); the former attained 96%–98% at 1700 °C, whereas the latter were 79%–93%.

The packing fraction of ultrafine MgO particles in the green compact has been estimated by computer simulation; Kitaoka and Seki [11] found that the packing fraction by volume of cubic particles is 22%–59%. A slight difference in maximum packing fraction between our value (60.7%) and their calculated value (59%) can be explained by assuming that any deviation from the idealized state, i.e. uniformities of particle size and shape, results in a difference in packing density.

It is noteworthy that 96%–98% relative density can be obtained by firing the compacts with primary particle sizes of 10–50 nm up to 1700 °C. The densification behaviour of MgO compacts will be discussed again after these microstructures are observed by SEM.

3.3. Microstructure development of MgO compact during firing

The microstructures of Compacts A(11), B(25), D(44) and G(261) without firing (Fig. 3) and with firing up to

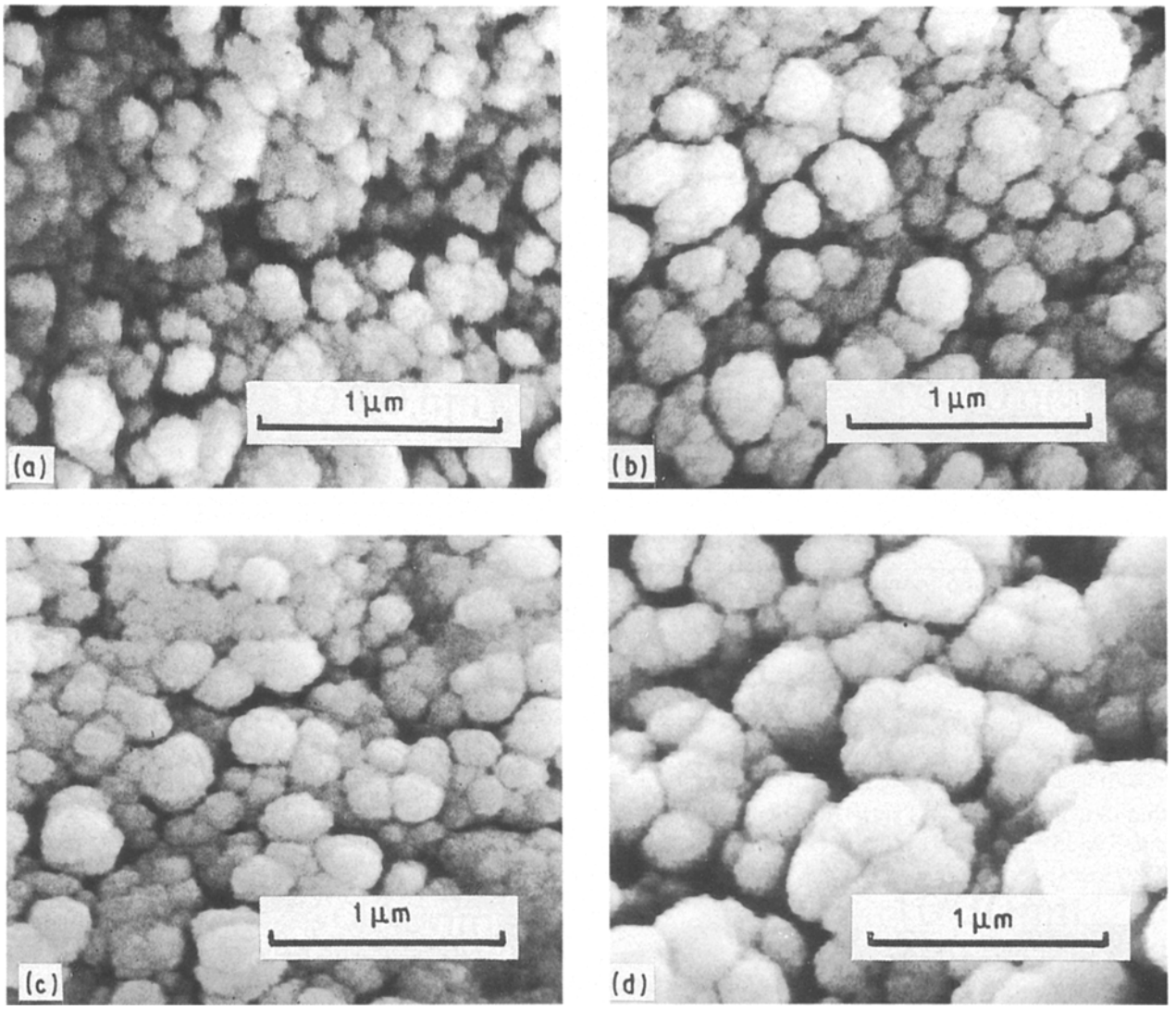

Figure 3 Scanning electron micrographs of green MgO compacts. (a) Compact A(11), (b) Compact B(25), (c) Compact D(44), (d) Compact G(261).

1200 °C (Fig. 4), 1400 °C (Fig. 5), 1500 °C (Fig. 6) and 1700 °C (Fig. 7) are shown in this section.

3.3.1. Microstructure of green MgO compact

The microstructure of sintered MgO compact may be affected by the packing state of primary particles in the green MgO compact; thus the microstructure of each green MgO compact was examined by SEM; the results are shown in Fig. 3. The overall trend revealed that primary particles were coagulated to form spherical agglomerates with diameters of 0.1–0.5 μm; the agglomerate size became larger with increasing primary particle size. Moreover, the agglomerates in Powder A(11) coagulated in a way which created wide interstices between them.

The following information was obtained from the above observation: (i) primary particles in the range 11–261 nm easily form spherical agglomerates, and (ii) the agglomerate size becomes larger with increasing primary particle size. The agglomeration of primary particles in MgO powder may occur spontaneously by the electrostatic and van der Waals forces [12]. The formation of larger agglomerates, which occurs with increasing primary particle size, is attributed to the coagulation of larger primary particles, regardless of the decrease in the number of primary particles within agglomerates.

The agglomeration of ultrafine MgO powder has also been reported by Nishida *et al.* [8], who stated that the primary particles with sizes below 20 nm form "hard" agglomerates and that these agglomerates start to fracture at ~30 MPa. In general, the fracture strength, S_p, of a compact can be calculated from the following equation [13]

$$S_p = S_0 e^{-bp} \quad (3)$$

where S_0 is the strength at zero porosity, P is porosity and b is a constant. When the data on porosity ($P = 0.76$) of Nishida *et al.* [8] and our previous data ($S_0 = 185$ MPa, $b = 6.0$) [14] are incorporated into Equation 3, S_p becomes only 1.9 MPa. The discrepancy between the measured strength (~30 MPa) and the calculated strength (1.9 MPa) demonstrates that the presence of dense agglomerates contributes to enhancing the mechanical strength up to ~30 MPa.

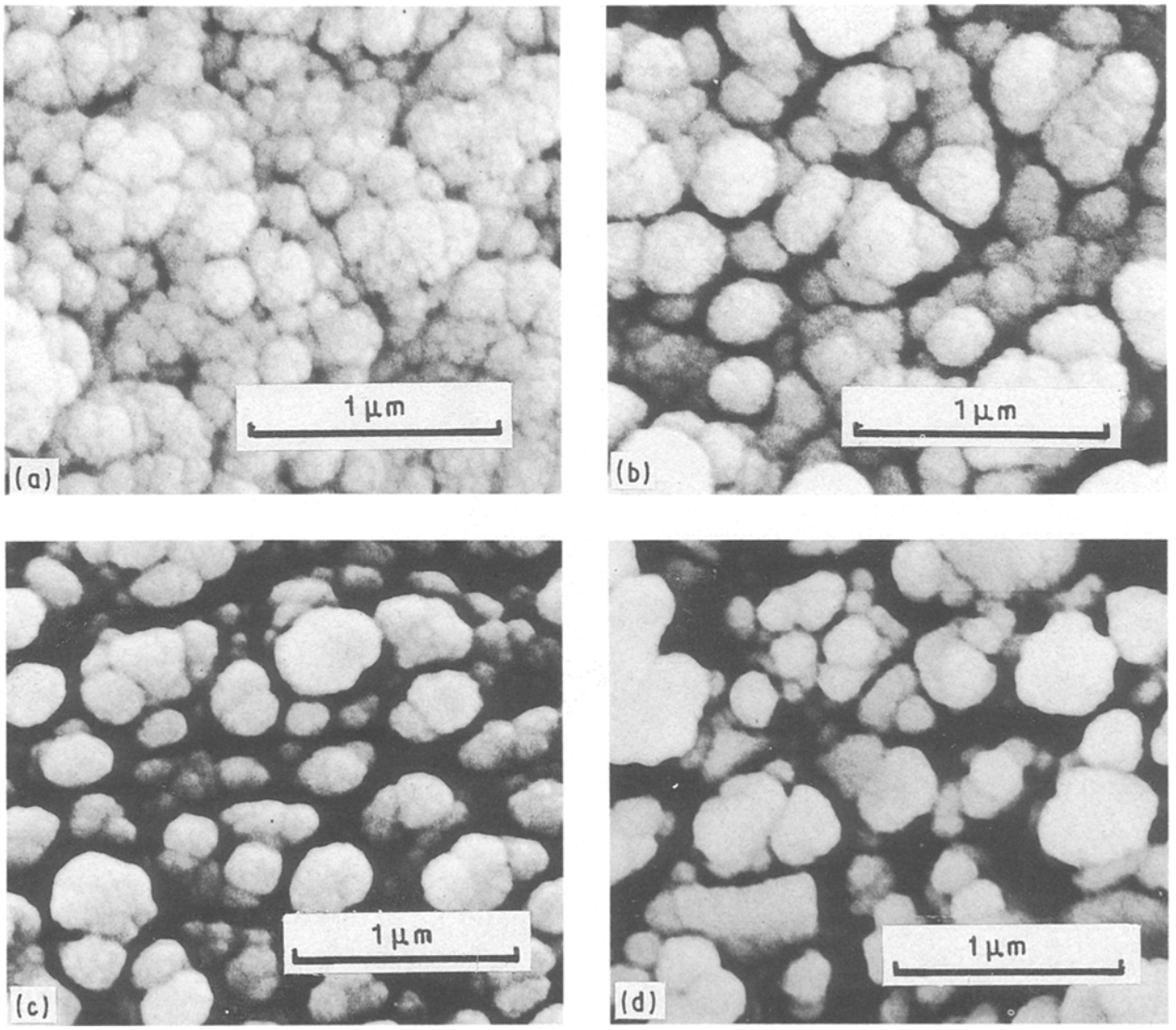

Figure 4 Scanning electron micrographs of MgO compacts fired to 1200 °C. (a) Compact A(11), (b) Compact B(25), (c) Compact D(44), (d) Compact G(261).

3.3.2. Microstructures of MgO compacts fired up to 1200, 1400, 1500 and 1700 °C

The microstructure development during the firing of MgO compacts from 1200–1700 °C were investigated at a heating rate of 10 °C min^{-1}. The microstructure of MgO compacts fired to 1200 °C are shown in Fig. 4. Compact A(11) exhibited the particles with sizes of ~0.05 μm coagulated to form spherical agglomerates with diameters of ~0.2 μm. The microstructure of Compact B(25) was similar to that of Compact A(11); however, the spherical agglomerates in Compact B(25), whose diameters (~0.3 μm) were somewhat larger than those in Compact A(11), were surrounded by irregularly shaped pores. The microstructure of Compact D(44) was composed of spherical agglomerates (diameter 0.1–0.3 μm) which were separated by the wide interstices. Compact G(261) showed spherical particles/grains, diameter 0.1–0.5 μm, which were packed randomly.

A comparison of the above results with those of green MgO compacts leads to the following conclusions: (i) the interstices between agglomerates/grains become wider when MgO compacts with larger primary particles are fired, and (ii) little change in agglomerate/grain size is observed after the firing of a green MgO compact. Conclusion (i) suggests that the sintering of primary particles within agglomerates occurs preferentially over the sintering between agglomerates [15]; very narrow interstices between agglomerates/grains are observed in Compact A(11), which proves the progress in simultaneous sintering within and between agglomerates during firing. Conclusion (ii) suggests that the coalescence of agglomerates/grains may be inhibited by the migration of pores along agglomerates/grains [16].

The microstructures of MgO compacts fired to 1400 °C are shown in Fig. 5. The microstructure of Compact A(11) showed that spherical agglomerates/grains with diameters 0.1–0.3 μm were in close contact with one another. The spherical agglomerates/grains were also present in Compact B(25) and had diameters of 0.1–0.5 μm: they stuck together randomly and were surrounded by irregularly shaped pores. The microstructure of Compact D(44) was composed of closely

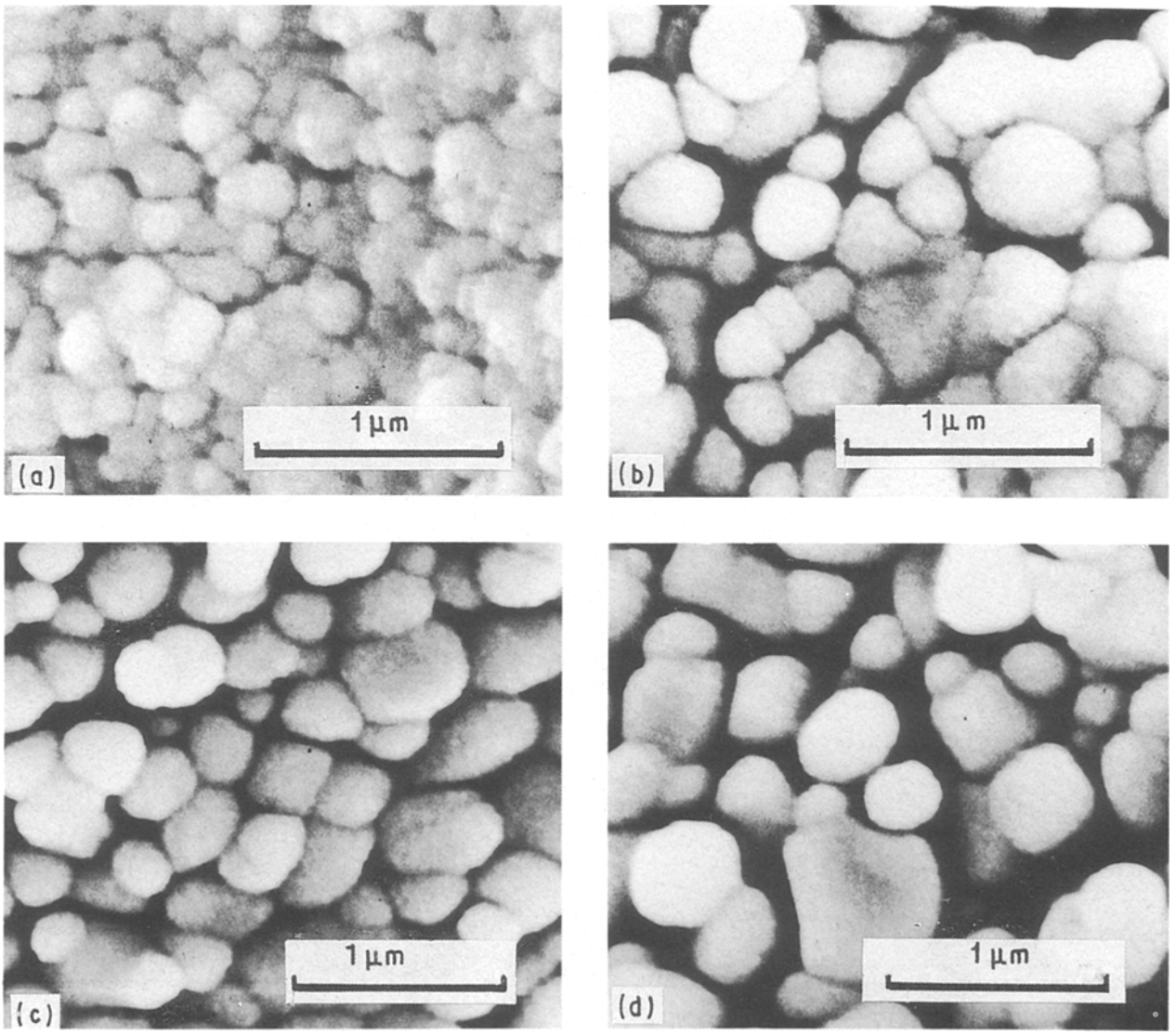

Figure 5 Scanning electron micrographs of MgO compacts fired to 1400 °C. (a) Compact A(11), (b) Compacts B(25), (c) Compact D(44), (d) Compact G(261).

packed spherical agglomerates/grains with diameters of ~0.5 μm, whereas that of Compact G(261) was composed of grains with sizes of 0.3–0.8 μm.

The agglomerates/grains in Compacts A(11) and D(44) show more uniform packing than those in Compacts B(25) and G(261). The uniform packing of agglomerates/grains in Compact A(11) is achieved by the effective elimination of pores along agglomerates/grains without pore growth, whereas that in Compact D(44) may occur by the rearrangement of the agglomerates/grains during firing. Here the agglomerate/grain sizes (0.1–0.3 μm) in Compact A(11) are smaller than those (1–5 μm) reported previously [7], indicating that the difference in green relative density, i.e. 36.5% and ~ 50%, respectively, affects the agglomerate/grain growth. The irregular packing of agglomerates/grains in Compact B(25) may be formed by the preferential sintering within agglomerates over the sintering between agglomerates. In the case of Compact G(261), the preferential sintering within agglomerates over that between agglomerates serves to create wide interstices after firing.

The microstructures of Compacts A(11) to G(261) fired to 1500 °C are shown in Fig. 6. The microstructures in Compacts A(11) to D(44) showed that polyhedral grains were closely in contact with one another and that the grain size decreased with increasing the primary particle size. The microstructure of Compact G(261) showed that pores were present between the polyhedral grains.

The above results reveal that most of the agglomerates change into grains at 1500 °C by the removal of pores within agglomerates. In the case of Compact A(11), for example, 4.5×10^7 primary particles (11 nm) are found from calculation to coalesce into a grain with an average size of 3.9 μm. The number of these primary particles is much more numerous than in the case (~200) of Compact G(261). Because the grains formed by the coalescence of a larger number of primary particles contain larger numbers of lattice defects, these defects may become the driving force for promoting grain growth.

The microstructures of Compacts A(11) to G(261) fired to 1700 °C are shown in Fig. 7. The microstructures of Compacts A(11) and B(25) were composed of closely packed polyhedral grains with sizes of 10–50 μm. The microstructure of Compact D(44) showed that the polyhedral grains with sizes of

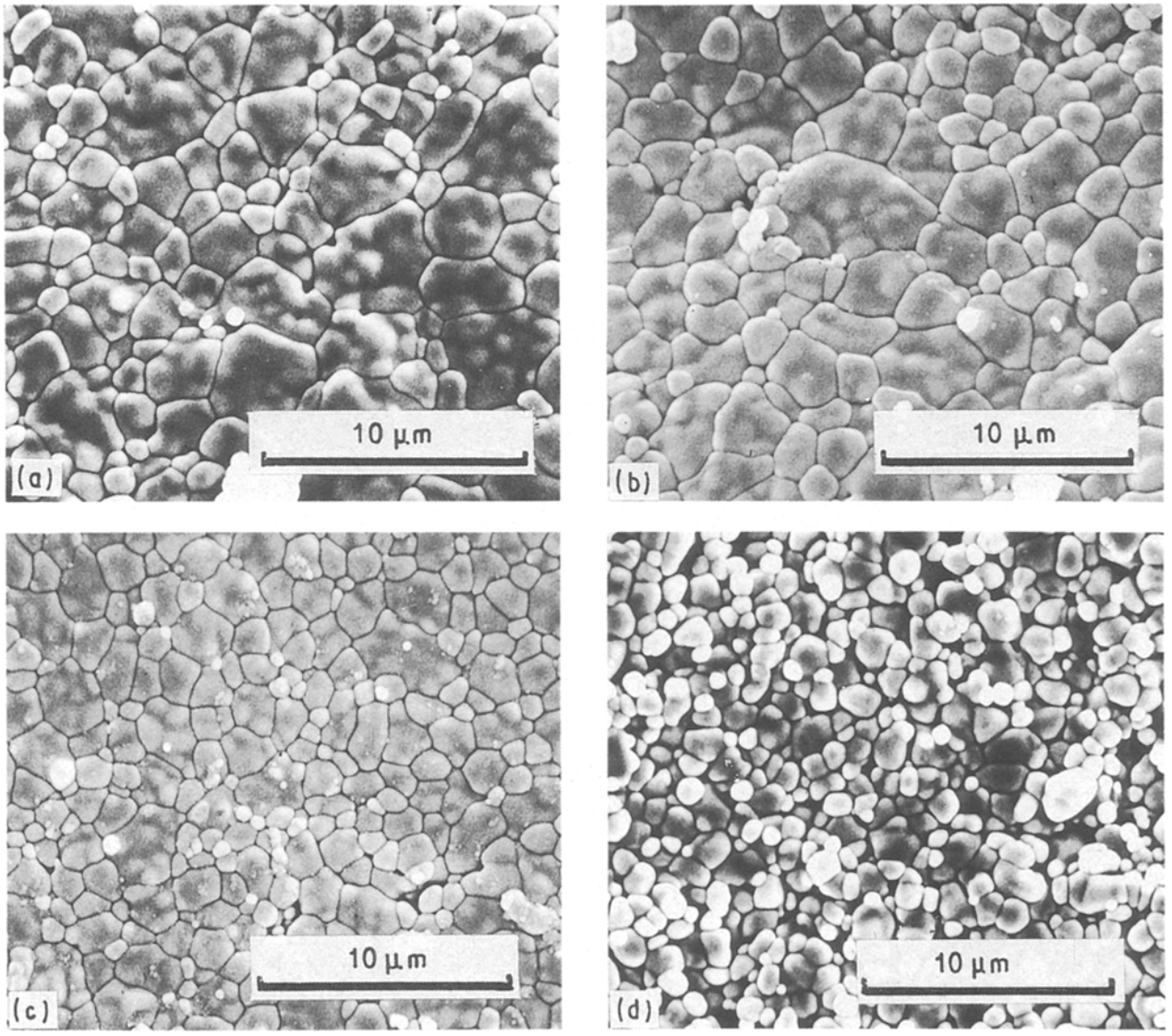

Figure 6 Scanning electron micrographs of MgO compacts fired to 1500 °C. (a) Compact A(11), (b) Compact B(25), (c) Compact D(44), (d) Compact G(261).

10–20 μm were packed closely; pores were present not only on grain boundaries but also within grains. Moreover, the microstructure of Compact G(261) was composed of polyhedral grains with sizes 1–5 μm and of pores on grain boundaries.

The uniform microstructures, i.e. uniform grain size and small numbers of pores, are formed by firing the compacts with primary particle sizes of 10–50 nm; however, pores remain not only on grain boundaries but also within grains. The presence of pores within grains suggests that the grain-boundary migration may occur more rapidly than the pore migration [17].

3.4. Relationship between crystallite/grain sizes and relative density

The relative densities are plotted against the crystallite sizes (10–500 nm) and grain sizes (over 500 nm), measured by XRD-T and SEM, respectively; the crystallite sizes roughly correspond to the particle sizes within agglomerates. Results are shown in Fig. 8; here the agglomerate sizes (100–500 nm) are not plotted in the figure, because of the difficulty in quantitative analysis. The relative density of Compact A(11) rose linearly from ~40% to 70% as crystallite sizes increased from 20 nm to 50 nm; when the relative density increased from 70% to ~95%, the grain size increased rapidly from $\sim 5 \times 10^2$ nm to $\sim 2 \times 10^4$ nm. Similar results were also obtained for the relative densities of Compacts B(25), C(32) and D(44); however, these crystallites/grains grew more rapidly than those in Compact A(11). The relative densities of Compacts E(57), F(107) and G(261) increased from ~50% to ~70% without appreciable crystallite growth; they increased from ~70% to ~90% with a marked grain growth from $\sim 5 \times 10^2$ nm to $\sim 5 \times 10^3$ nm.

The above results show that the rapid crystallite/grain growth starts to occur when the relative density exceeds 65%–70%. These values lie in the range between random close packing (~65%) [18] and theoretical closest packing (74.05%) [11]. This fact suggests that once the grains, formed by the sintering of primary particles within agglomerates, are rearranged to show the closer packing (~70%), the grain

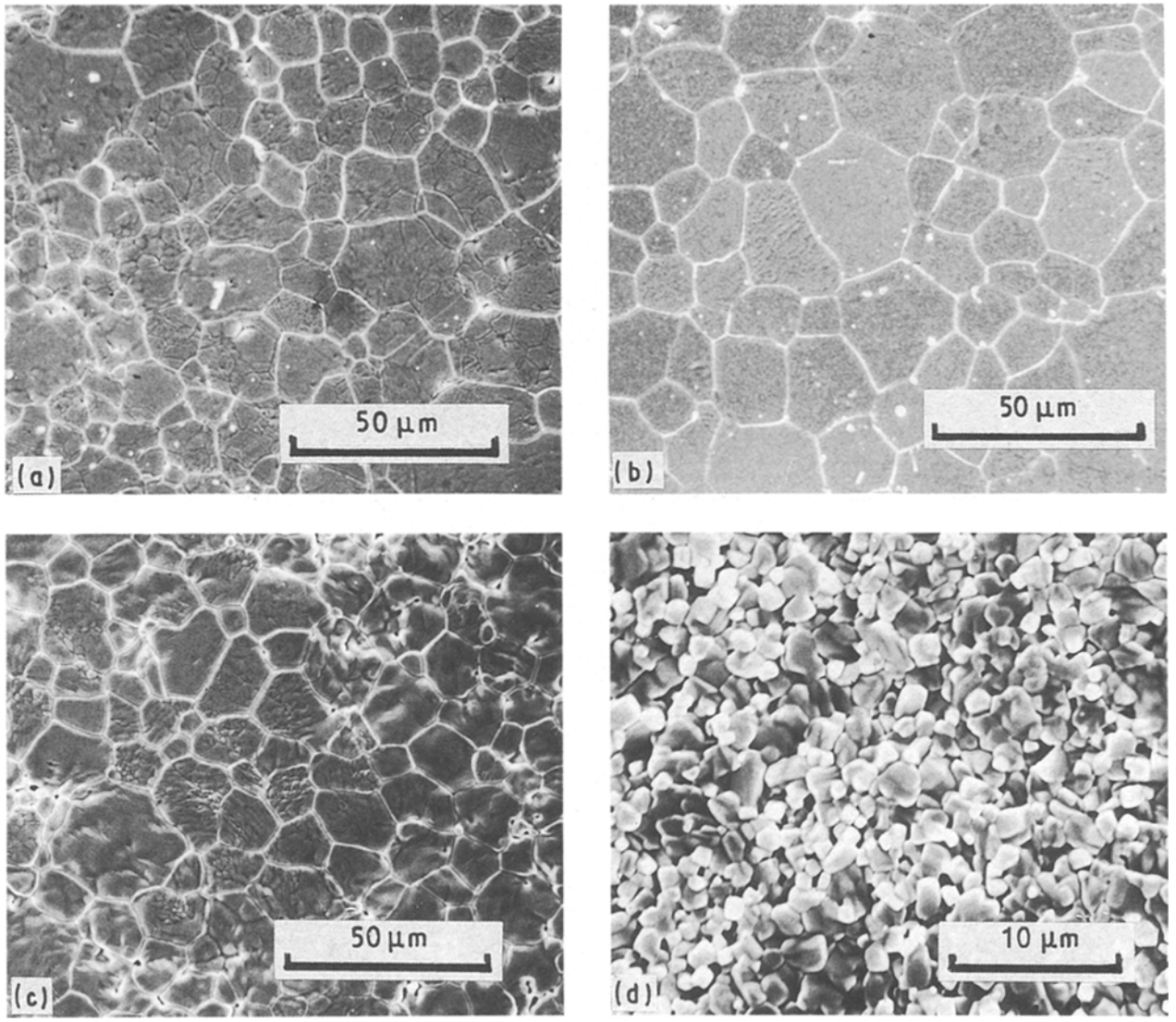

Figure 7 Scanning electron micrographs of MgO compacts fired to 1700 °C. (a) Compact A(11), (b) Compact B(25), (c) Compact D(44), (d) Compact G(261).

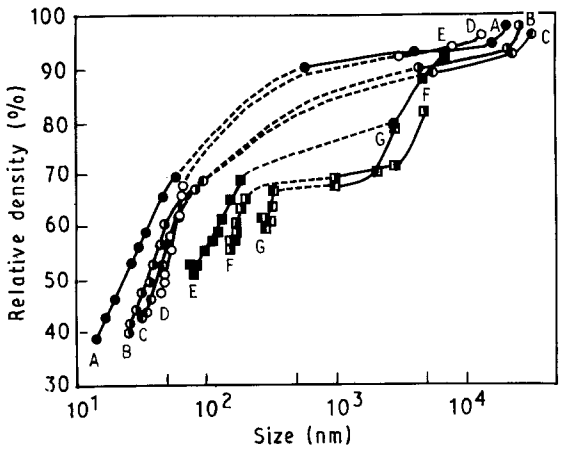

Figure 8 Relationship between crystallite/grain sizes and relative density during the firing of MgO compacts in the range 600–1700 °C. A to G: Compacts A(11) to G(261). (●, ◑, ◐, ○); Crystallite sizes, (■, ◨, ◧, □) Grain sizes.

growth starts to be promoted by the mass transfer via the contact area of these grains.

On the basis of the results in Figs 1 –8, the schematic diagrams of densification and microstructure developments of MgO compacts are shown in Fig. 9. The agglomeration in original MgO powder may occur due to the spontaneous coagulation of primary particles (i).The densification of MgO compact with the primary particle size of ~11 nm proceeds by the simultaneous sintering within and between agglomerates (ii), which forms a microstructure with closely-packed grains (iii). The densification of MgO compact with the primary particle size of ~44 nm proceeds by the volume reduction of agglomerates on the basis of preferential sintering within agglomerates over the sintering between agglomerates (iv); after these agglomerates are rearranged towards closer packing (v), the rapid sintering occurs to form the microstructure with closely packed grains (vi). Furthermore, the densification of MgO compact with the primary particle size of 50–261 nm may be due to the irregular packing of agglomerates (vii) via route (iv); the sintered MgO compact contains many pores on grain boundaries (viii).

As shown above, the densification of MgO compact with the primary particle size of ~10 nm proceeded in two steps: (1) the sintering within agglomerates, and

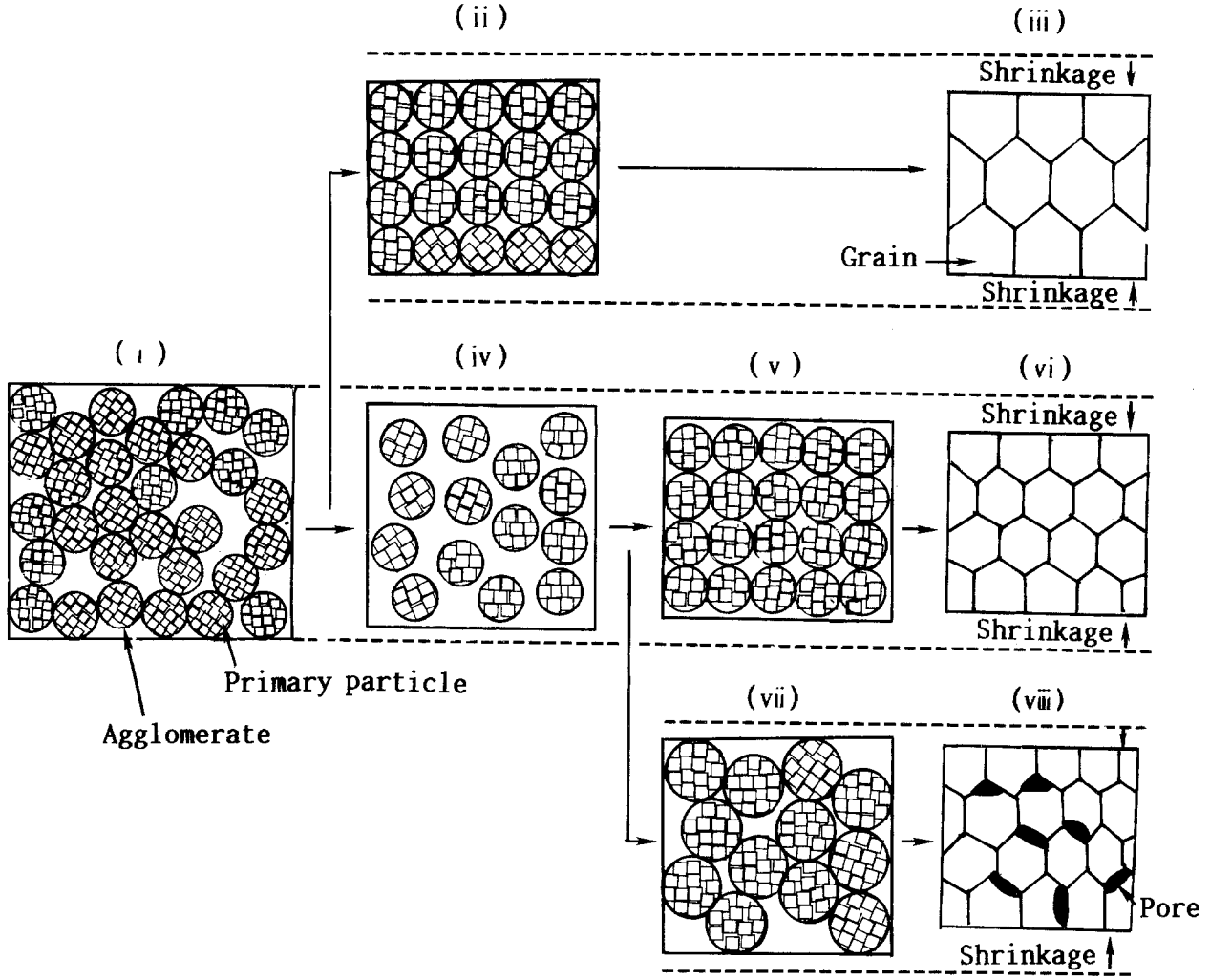

Figure 9 Models for the sintering of submicrometre MgO particles during firing. (i) Packing of agglomerates in MgO compact. (ii) Uniform array of agglomerates (the sintering within and between agglomerates). (iii) Close packing of grains. (iv) Volume reduction of agglomerates due to the preferential sintering within agglomerates over the sintering between agglomerates. (v) Rearrangement of agglomerates. (vi) Close packing of grains. (vii) Random packing of agglomerates after the coalescence of smaller agglomerates. (viii) Remaining of pores on grain boundaries. Densification routes: (1) primary particle size, 11 nm, (i) → (ii) → (iii); (2) primary particle size, 44 nm, (i) → (iv) → (v) → (vi); (3) primary particle sizes, ~50–261 nm, (i) → (iv) → (vii) → (viii).

(2) the sintering between agglomerates/grains. These two effects reduce with increasing primary particle size up to 44 nm and, instead, (3) the rearrangement of agglomerates/grains contributes to densifying the MgO compact. These three types of densification became less complete with further increase in primary particle size up to 261 nm.

4. Conclusions

The effect of primary particle size on densification and microstructure development has been examined by firing the MgO compacts to 1700 °C (heating rate 10 °C min^{-1}). The following results were obtained.

1. The agglomerates of original MgO powder may be formed by the spontaneous coagulation of primary particles. The densification of MgO compact during the firing proceeded in three steps: (i) sintering within agglomerates, (ii) sintering between agglomerates and/or grains, and (iii) the rearrangement of agglomerates and/or grains.

2. The densification of MgO compact with a primary particle size of 11 nm proceeded chiefly in two steps: the sintering within agglomerates and that between agglomerates/grains. With increasing primary particle size up to 44 nm, however, these two effects decreased; here the rearrangement of agglomerates/grains contributes to densifying the MgO compact. All three types of densification became less complete with further increases in primary particle size up to 261 nm.

3. The relative densities of the MgO compacts with smaller primary particle sizes (11–44 nm) became 96%–98% when the compacts were fired to 1700 °C.

Acknowledgements

The authors thank Ube Industries Ltd for providing sample powders. This research was partly supported by grants-in-aid from the Foundation "Hattori-Hokokai".

References

1. N. NAKANISHI, M. TAKANO and H. KUMITO, *J. Jpn Soc. Powder and Powder Metall.* **24** (1977) 1.
2. T. HATTORI, H. MATSUMOTO and J. MOHRI, *J. Mater. Sci. Lett.* **2** (1983) 503.

3. T. J. GARDNER and G. L. MESSING, *Amer. Ceram. Soc. Bull.* **63** (1984) 1498.
4. A. NISHIDA, K. YOSHIDA, H. IGARASHI and W. KOBAYASHI, in "Advanced Ceramics 21, Ceramic Powder Science" edited by G. L. Messing, K. S. Mazdiyasni, J. W. McCauley and R. A. Haber (American Ceramic Society, Columbus, OH, 1987) p. 265.
5. A. KATO, *Ind. Ceram.* **7** (1987) 105.
6. T. WATARI, K. NAKAYOSHI and A. KATO, *J. Chem. Soc. Jpn* **1985** (1985) 790.
7. K. ITATANI, M. NOMURA, A. KISHIOKA, M. KINOSHITA, *J. Mater. Sci.* **21** (1986) 1429.
8. A. NISHIDA, K. YOSHIDA, H. IGARASHI and W. KOBAYASHI, in "Advanced Ceramics 21, Ceramic Powder Science" edited by G. L. Messing, K. S. Mazdiyasni, J. W. McCauley and R. A. Haber (American Ceramic Society, Columbus, OH, 1987) p. 271.
9. R. L. FULLMAN, *Trans. AIME* **197** (1953) 447.
10. K. ITATANI, K. KOIZUMI, F. S. HOWELL, A. KISHIOKA and M. KINOSHITA, *J. Mater. Sci.* **23** (1988) 3405.
11. T. KITAOKA and Y. SEKI, *Seramikkusu Ronbunshi* **96** (1988) 585.
12. H. RUMPF and H. SCHUBERT, in "Ceramic Processing before firing", edited by G. Y. Onoda and L. L. Hench (Wiley, New York, 1978) p. 61.
13. W. DUCKWORTH, *J. Amer. Ceram. Soc.* **36** (1953) 68.
14. K. ITATANI, S. SATO, F. S. HOWELL, A. KISHIOKA and M. KINOSHITA, *Seramikkusu Ronbunshi* **97** (1989) 593.
15. W. H. RHODES, *J. Amer. Ceram. Soc.* **64** (1981) 19.
16. C. H. HSUEH and A. G. EVANS, *Acta Metall.* **31** (1983) 189.
17. R. J. BROOK, *J. Amer. Ceram. Soc.* **52** (1969) 56.
18. W. S. JODREY and E. M. TORG. *Phys. Rev.* **A32** (1985) 2347.

Received 2 September 1991
and accepted 7 May 1992